

Effect of Beam Oscillation on Microstructure and Tensile Property of Electron Beam-Welded Commercially Pure (CP) Titanium

Jeetendra Kumar Singh¹ · Gour Gopal Roy¹ · Jyotsna Dutta Majumdar¹ 

Received: 9 July 2022 / Accepted: 6 October 2022 / Published online: 7 November 2022
© The Indian Institute of Metals - IIM 2022

Abstract In the present study, electron beam welding of commercially pure titanium has been carried out at an accelerating voltage of 60 kV, current of 40 mA, and beam speed of 900 mm/min without beam oscillation and with beam oscillation having varied oscillation diameter of 0.5–1.5 mm. The microstructure of the fusion zone shows the formation of Widmanstätten martensite and feathery α -titanium phase as compared to the fine acicular α -phase in the base metal. The phase analysis shows the presence of only the α -titanium phase in the fusion zone. The residual stress induced in the joint increases (1069–1366 MPa) with the increase in oscillation diameter as compared to static beam (877 MPa) and base metal (622 MPa). Due to electron beam welding without beam oscillation, there is a marginal reduction in yield strength (465–462 MPa), ultimate tensile strength (626–623 MPa), and % elongation (18.2–14%) as compared to as-received titanium. The introduction of beam oscillation of varied oscillation diameter leads to a marginal reduction in yield strength (457–452 MPa) and ultimate tensile strength (623–622 MPa), whereas, the percentage elongation increases (14–18%) with an increase in oscillation diameter as compared to the static beam. The fractography of the failed surfaces shows a mixed-mode fracture.

Keywords Titanium · Electron beam welding · Tensile strength · Beam oscillation

1 Introduction

Titanium alloys possess an outstanding combination of properties like high specific strength, good fatigue life, and excellent corrosion resistance. As a result, they have wide-ranging applications in the aerospace and marine sector. CP titanium has lower strength than other alloys, but it is the alloy of choice for applications requiring corrosion resistance, and it has better elevated temperature creep resistance and is less expensive than the other titanium alloys [1]. Conventionally, tungsten inert gas welding (TIG) and metal inert gas welding (MIG) are employed for welding titanium and its alloys [2]. GTAW of Ti and its alloys has been studied in detail [3–5] but its use is limited due to higher heat input, whereas GMAW is not used extensively. Friction stir welding (FSW) of titanium and its alloys causes excessive tool wear [6]. Laser and electron beam welding (EBW) is a high energy density beam welding technique which is having higher energy efficiency and several advantages like faster processing speed and negligible heat-affected zone. However, due to a lack of extensive work and reported literature they are not commercially used for welding titanium. Furthermore, electron beam welding is having the additional advantage of the development of a contaminant-free weld zone without the requirement of additional shielding gas. The problem of beam reflection from the molten pool encountered in LBW is not so severe in EBW [7]. Compared to LBW, EBW has better energy absorption independent of material and surface conditions and the capability of performing deeper penetration weld with a higher aspect ratio and relatively less heat-affected zone. Yunlian et al. [8] attempted to weld Ti by TIG, LBW, and EBW. A serrate and regular plate-like structure appeared in FZ for EBW,

✉ Jyotsna Dutta Majumdar
jyotsna@metal.iitkgp.ernet.in;
duttamajumdarjyotsna@gmail.com

¹ Metallurgical and Materials Engineering Department, IIT Kharagpur, Kharagpur, India

while a fine acicular structure was observed for LBW. Relatively larger α -phase structures in EBW FZ were due to lower cooling rates in EBW with respect to LBW. Micro-hardness was found to be lowest in the weld zone in the case of EBW. The parameters usually applied in EBW include accelerating voltage, beam current, scan speed, and beam oscillation [9, 10]. In the past, several studies have been undertaken to understand the influence of beam acceleration voltage and scan speed on the characteristics and properties of electron beam-welded titanium [11–13]. However, there is a limited report in the literature showing the effect of beam oscillation on the characteristics and properties of CP titanium. Gupta et al. [14] studied the mechanical properties at room temperature as well as at a cryogenic temperature of as-received CP titanium as well as electron beam-welded joints. The strength of the weldment as well as parent metal increased with a decrease in temperature. Weld efficiency > 95% at all the temperatures (ambient, 77 K, 20 K) was observed. Optical microscopy revealed the presence of single phase α in parent metal, which transformed to Widmanstätten martensitic structure with feathery morphology in the weld. An increase in dislocation density near the failure tip of the tensile test specimen and the presence of dimples were observed indicating ductile failure/ sufficient amount of ductility even at 20 K. Wang and Wu [15] investigated the effect of linear beam oscillation on microstructural refinement in the fusion zone and β -stabilizing elements segregation in Ti-6Al-4 V joints. Fu et al. [16] investigated the BOP joining of 50-mm-thick TC4-DT alloy with an oscillated beam using the EBW process. They reported that the application of beam oscillation improved the weld morphology and increased the width of the weld. They also concluded that the beam oscillation produced a more homogeneous microstructure due to improved fluidity and solidification of molten metal. It was found that the joints prepared with beam oscillation have better fatigue properties as compared to the static beam counterparts. Dinda et al. [17] studied the effect of beam oscillation on electron beam welding of DP600 steel to Al 5754 alloy and reported an optimum value of beam oscillation which reduced the defect content in the weld zone. They also concluded that beam oscillation diameter higher or lower than the optimum value may increase the porosity in the weld zone. Kar et al. [18] studied the effect of beam oscillation on electron beam welding of Ti6Al4V alloy. They studied the effect of circular beam oscillation on microstructure evolution and its influence on the mechanical properties of EBW of Ti6Al4V. Kar et al. [18] reported joints prepared with beam oscillation to show better notch toughness and higher %elongation due to the evolution of refined homogeneous microstructure in the weld zone. They also reported an

increase in residual stress due to beam oscillation but it was still less than TIG and laser welding. From the above discussion, it is clear that the effect of beam oscillation has been studied mainly in Ti6Al4V whereas we did not find any literature on the effect of beam oscillation on the EBW of CP titanium.

In the present study, electron beam welding of similar titanium joints has been carried out using a constant acceleration voltage, beam current, scan speed, and its effect on the microstructure and tensile strength has been carried out. Furthermore, attempts have been made to understand the effect of beam oscillation diameter on the microstructure, microhardness, and tensile properties of the CP titanium joints.

2 Experimental

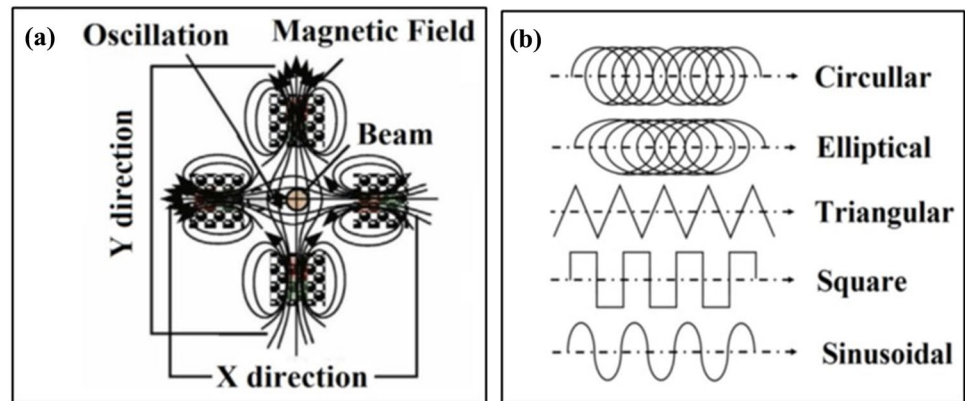
2.1 Materials and Methods

In the present study, commercially pure (CP) titanium sheets of dimensions 60 mm × 50 mm × 3 mm in the cold-rolled and annealed state were used as a workpiece for welding. The composition (in weight %) of the as-received titanium as obtained from X-ray fluorescence spectroscopy (XRF) is Al—0.2%, Fe—0.06%, Si—0.04%, Ni—0.01%, Mn—0.01%, Cr—0.01%, and the rest is Ti. Before the electron beam welding (EBW), the samples were mechanically polished up to a roughness of 5 μm . Electron beam welding was carried out using an electron beam welding machine with a capacity of 80 kV voltage, and 12 kW power (make BARC, India) using an optimum process parameter of 60 kV acceleration voltage, 40 mA current, 900 mm/min welding speed, and work chamber vacuum level of 5×10^{-5} mbar. The optimum parameters used were derived through an extensive study of the effect of process parameters on the microstructure and defect density of weld zone and heat-affected zone and the parameters reported were the same corresponding to the formation of a defect-free weld zone with full penetration (c.f. Table 1). Edge preparation for the butt joint was performed to make the mating faces of the two-samples parallel to each other by a milling operation. Before welding, the workpieces were cleaned properly with acetone to remove any dirt or grease. From Table 1, it may further be noted that the only variable for electron beam welding was the beam oscillation diameter which varied from 0 to 1.5 mm. Figure 1 shows the schematic of beam oscillation using an applied magnetic field and different types of oscillation patterns commonly used in EBW [11]. Circular beam oscillation with a frequency of 300 Hz was selected in the present study.

Table 1 Summary of electron beam welding parameters used in the present study

S. No	Sample Id	EB welding parameter (Kept constant for all samples)	Beam oscillation diameter (mm)	Other oscillation parameters
1	Joint 1	Voltage = 60 kV	0	Frequency—300 Hz
2	Joint 2	Beam current = 40 mA	0.5	Pattern—Circular Beam focus—On the surface
3	Joint 3	Welding speed = 900 mm/min	1.0	
4	Joint 4	Work Chamber vacuum = 5×10^{-5} mbar	1.5	

Fig. 1 a Beam oscillation in electromagnetic fields and b different oscillation patterns of electron beam [11]



2.2 Microhardness Measurement

The microhardness of as-received and electron beam (EB)-welded CP titanium was measured using Vickers microhardness tester (UHL-VMHT 001, Germany) at an applied load of 100 gf and dwell time of 10 s following ASTM E384-17 standard and an average of five measurements at each point has been reported. The microhardness was measured starting from the base metal to HAZ to the fusion zone till the base material was reached. The distance between two consecutive indents was kept as 0.5 mm. The Vickers hardness was calculated using the following Eq. (1):

$$H_V = \frac{1.854P}{d_{avg}^2} \tag{1}$$

where P is the applied normal load in kgf and $d_{avg} = (d_1 + d_2)/2$, where d_1 and d_2 are the lengths in mm of the two diagonals of indentation.

2.3 Phase Analysis and Residual Stress Measurement

Phase analysis was performed by X-ray diffraction technique using an X-ray diffractometer (Model No.: D8 Advance, Make: Bruker, Germany), operating at a voltage of 40 kV and current of 25 mA using Cu $K\alpha$ radiation. Spectra were analyzed using X’pert High Score software.

Residual stress was measured using a stress goniometer attached to an X-ray diffraction unit. Residual stress in the joints was measured in the center of the fusion zone, and an average of three measurements in each sample was reported. The obtained results were analyzed in X’pert stress software following the $\sin^2\psi$ method. For Ti joints, $2\theta = 70.263$ degrees having hkl of (3 1 0) were chosen for the calculation of residual stress. Here, the peak selection is based on the higher diffraction angle as it increases the precision of the method selected.

2.4 Tensile Test

Tensile testing was carried out in such a fashion that the weld zone is in the middle of the gauge length of the test specimen and the welding direction is perpendicular to the test specimen. Tensile test was carried out using a universal testing machine with a maximum capacity of 100 kN make Instron® (model: 8862) at room temperature following ASTM E8/E8m-15a (2015). Total length of the specimen is 100 mm whereas the gauge length is 25 mm. Testing was conducted by displacement-controlled method with 0.5 mm/min crosshead velocity. Four specimens were tested under each set of parameters and an average of four readings were reported. Tensile test results were recorded in terms of 0.2% offset yield strength, ultimate tensile strength, and % elongation to rupture.

3 Results and Discussion

3.1 Microstructural Evolution

Figure 2 (a–e) shows the optical micrographs of the (a) base metal, and fusion zone of EB-welded CP titanium joints (b) joint 1 (c) joint 2 (d) joint 3 (e) joint 4 processed with parameters given in Table 1. From Fig. 2(a), it may be noted that the microstructure of the base metal consists of fine equiaxed alpha grains. The fusion zone microstructure (Fig. 2 (b–e)) shows the formation of a Widmanstatten-type martensitic structure due to the higher cooling rate associated with EBW. The alpha phase present in the weld zone shows a feathery type of morphology as compared to fine equiaxed in as-received CP titanium [13, 14]. The application of beam oscillation tends to make the microstructure more uniform. The feathery α -phase is found to reduce with the increase in the beam oscillation diameter, and it is absent in the sample welded with a maximum oscillation diameter of 1.5 mm (Fig. 2e). Gupta et al. [13] also reported the increase in microhardness of the weld zone due to the presence of feathery morphology of α -titanium in the weld zone. The introduction of beam oscillation also causes the refinement of the microstructure, and the degree of refinement increases with the increase in beam oscillation diameter. Kar et al. [18] also reported a similar effect of beam oscillation on microstructure.

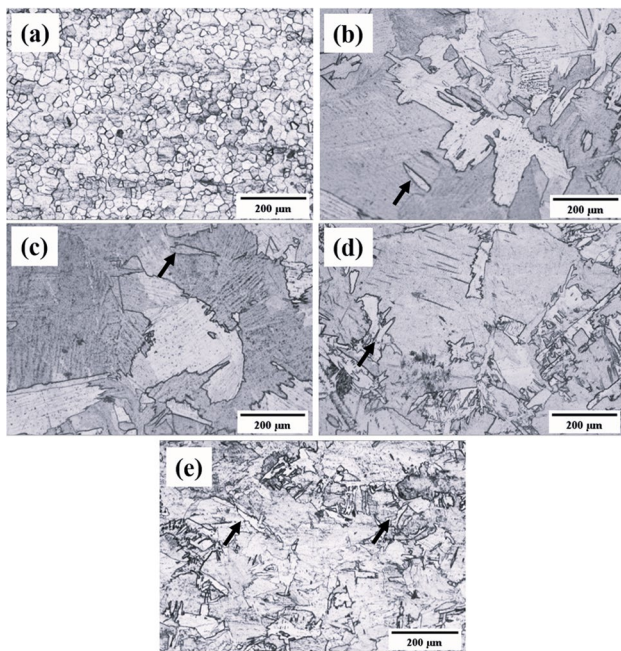


Fig. 2 Optical micrographs of the **a** base metal, and weld zone with **b** no beam oscillation (Joint 1) and with beam oscillation using the oscillation diameter of **c** 0.5 mm (Joint 2) **d** 1.0 mm (joint 3) and **e** 1.5 mm (Joint 4)

3.2 Phase Analysis

The X-ray diffraction technique was used to identify the phases formed in the weld zone of CP titanium samples. Figure 3 shows the X-ray diffraction spectra obtained from the samples welded using different beam oscillations. The spectra confirm the presence of only the α -Ti phase in the weld zone. No new phase or presence of contaminants is noticed after electron beam welding. The lattice strain developed in EB-welded titanium was calculated from the analysis of peak broadening using the Scherrer formula [19]. The lattice strain in EB-welded samples (c.f. Table 2) has been found to vary from 0.2% to 0.25% as compared to 0.3% for as-received titanium and does not follow any specific trend.

Texture coefficients along all the planes are calculated from XRD data using the following formula (Fig. 4).

$$T_C(hkl) = \frac{I(hkl)/I_0(hkl)}{(1/N)[I(hkl)/I_0(hkl)]} \quad (2)$$

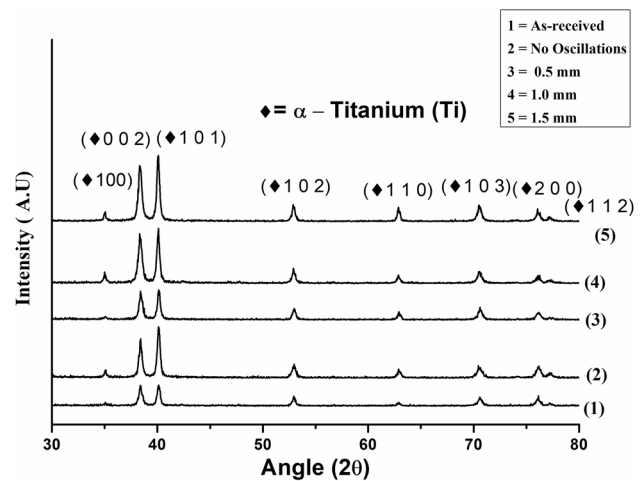


Fig. 3 X-ray diffraction profiles of the as-received CP titanium (plot 1) and EB-welded without beam oscillation (plot 2), and using oscillation diameters of 0.5 mm (plot 3), 1.0 mm (plot 4), and 1.5 mm (plot 5)

Table 2 Variation of lattice strain and residual stress developed in as-received and EB-welded CP titanium as a function of beam oscillation diameter

S. No	Beam oscillation dia. (mm)	Lattice strain (%)	Residual stress (MPa)
1	As-received	0.3	621 ± 22
2	0	0.23	877 ± 18
3	0.5	0.2	1069 ± 12
4	1	0.25	1116 ± 14
5	1.5	0.2	1366 ± 17

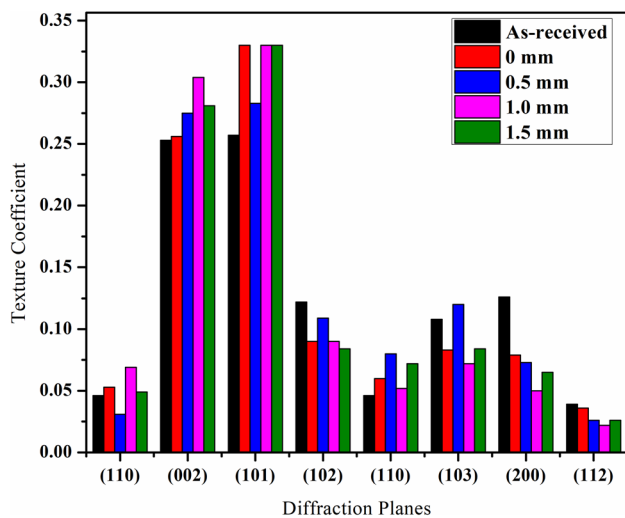


Fig. 4 Variation of texture coefficient along different planes for as-received and electron beam-welded CP titanium-welded using static and oscillated beams

where $T_c(h\ k\ l)$ is the texture coefficient along $(h\ k\ l)$ plane, I is the measured intensity, I_0 is standard intensity from JCPDS file, and N is the number of diffraction peaks.

From Fig. 4, it is clear that all the welded samples as well as base metal show strong texture along the (002) and (101) planes. The change in texture along the different planes is observed after EBW and with the application of beam oscillation but no specific trend is observed with the beam oscillation diameter. The variation in the intensity of α -titanium phase in XRD spectra is due to changes in the texture along the different planes with the process parameters.

3.3 Residual Stress Measurement

In the present study, the residual stress developed in the fusion zone is measured using a stress goniometer attached to an X-ray diffraction unit. Table 3 summarizes the residual stress developed in as-received and welded titanium processed using different beam oscillation diameters. The residual stress in the welded samples is measured at the center of the fusion zone. From Table 3, it may be

noted that for both the as-received and welded samples the residual stress is tensile in nature. The residual stress in the as-received titanium may be attributed to the fabrication process employed during the development of the sheet. The residual stress developed in the fusion zone of the electron beam-welded samples is tensile in nature which is in agreement with earlier reported literature. The value of the residual stress increases after electron beam welding. Residual stress also increases with the increase in the applied beam oscillation diameter. The value of the residual stress is 877 MPa for no oscillation, 1069 MPa for 0.5 mm beam oscillation, 1116 MPa for 1.0 mm beam oscillation, and 1366 MPa for 1.5 mm beam oscillation as compared to 621 MPa of as-received titanium. This increase in the residual stress with the beam oscillation diameter may be attributed to decreased heat input per unit length and increased cooling rate associated with the increase in beam oscillation diameter [18].

3.4 Evaluation of Microhardness

Microhardness of the weld zone and heat-affected zone of the EB-welded CP titanium processed using different beam oscillations was measured using a Vickers microhardness testing machine with an applied load is 100 gf and an indentation time of 10 s. Figure 5 shows the variation of microhardness of the electron beam-welded CP titanium processed with and without beam oscillation. The microhardness is measured starting from the base metal to HAZ to the fusion zone till the base material is reached. Based on the change in the microhardness of the fusion zone, the HAZ and base metal regions can be clearly distinguished. The base metal has a microhardness of 235 VHN which increases slightly in HAZ. The average microhardness in the HAZ is 245 VHN, and it does not vary much with the application of beam oscillation. The microhardness in the fusion zone increases sharply, and it is maximum for the sample-welded without beam oscillation (265 VHN). The application of beam oscillation tends to reduce the microhardness in the fusion zone, and it is reduced further with the increase in the beam oscillation diameter. The sample welded with a maximum oscillation

Table 3 Variation of tensile test parameter in electron beam-welded samples under varied beam oscillation

Specimen designation	Beam oscillation diameter	0.2% YS in (MPa)	UTS in (MPa)	Elongation (%)	Fracture location
Base alloy		465 ± 2	626 ± 3	18.2 ± 2	
Joint-1	0	462 ± 3	623 ± 2	14 ± 2	Joint
Joint-2	0.5	457 ± 2	622 ± 2	15 ± 2	Joint
Joint-3	1.0	446 ± 5	611 ± 5	16 ± 1	Joint
Joint-4	1.5	452 ± 2	622 ± 3	18 ± 1	Joint

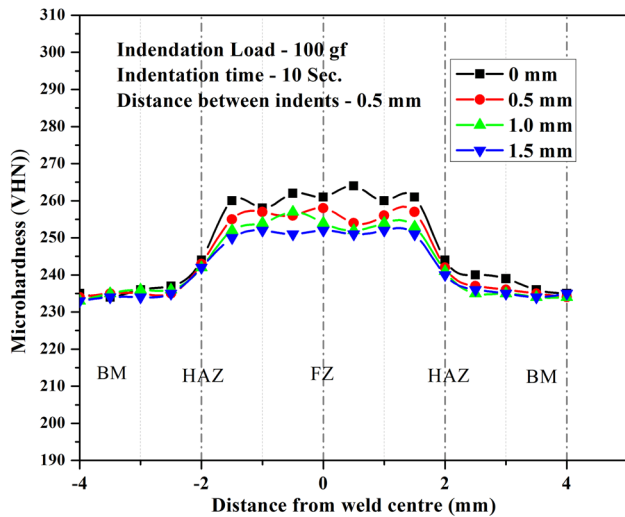


Fig. 5 Variation of microhardness across the different zones (base metal, HAZ, and FZ) of the as-received and EB-welded CP titanium processed static and oscillated beam of different beam diameters

diameter of 1.5 mm shows the minimum microhardness (250 VHN) in the fusion zone as compared to 265 VHN of un-oscillated and 235 VHN of as-received CP titanium. This decrease in microhardness with the increase in beam oscillation diameter may be attributed to the reduction in the feathery α - titanium phase (c.f. Figure 2) present in the fusion zone [13].

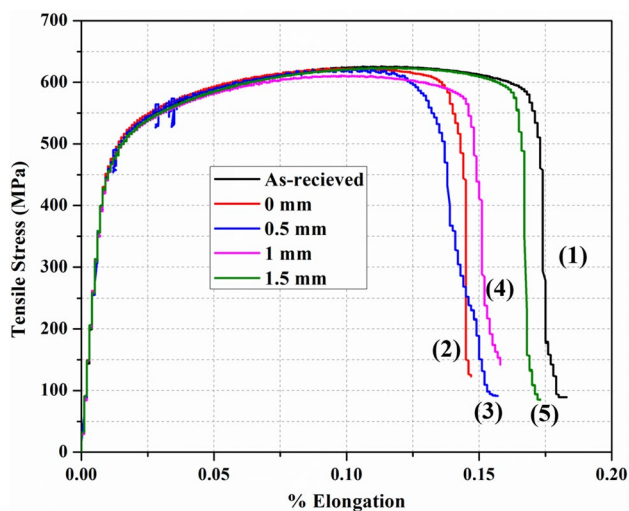


Fig. 6 Stress–strain diagram of CP titanium (plot 1) and same after EB welding without beam oscillation (plot 2) and with beam oscillation 0.5 mm (plot 3), 1.0 mm (plot 4), 1.5 mm (plot 5)

3.5 Evaluation of Tensile Property

Figure 6 shows the engineering stress–strain diagram of the as-received and EB-welded CP titanium processed with static beam and oscillated beam of different beam diameters. Notable parameters out of the stress–strain diagram like 0.2% YS, percentage elongation to rupture, and ultimate tensile strength (UTS) were computed and are presented in Table 3. From Table 3, it may be noted that in all the EB-welded samples, failure takes place in the weld zone. From Table 3, it may further be noted that the yield strength varies from 446 to 465 MPa and no specific trend in its variation with oscillation diameter is noticed. The UTS value, on the other hand, varies from 611 to 622 MPa and the maximum UTS is observed for the samples welded without beam oscillation. The joined prepared with 1.5 mm beam oscillation shows better YS and UTS as compared to 1 mm beam oscillation due to a more uniform and refined microstructure obtained with 1.5 mm oscillation diameter (Fig. 2). The variation of % elongation shows that there is a decrease in % elongation (18.2% to 14%) for the sample welded without oscillation. The introduction of beam oscillation tends to increase the % elongation, and it also increases with the increase in beam oscillation diameter. The sample welded with an oscillation diameter of 1.5 mm shows 18% elongation which is comparable to % elongation of as-received

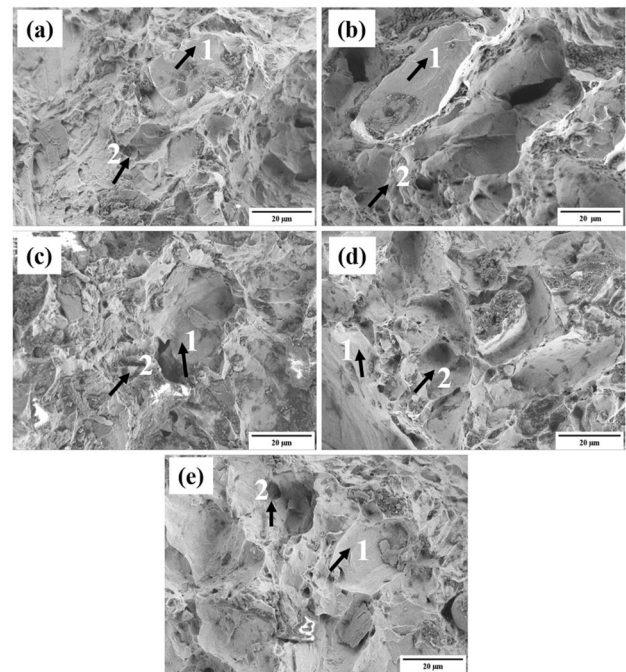


Fig. 7 Fractographs of the failed surfaces under tensile loading in a base metal, and the same after EBW b without any beam oscillation (Joint 1) and with beam oscillation using oscillation diameter of c 0.5 mm (Joint 2) d1.0 mm (joint 3) and e 1.5 mm (Joint 4)

CP titanium (18.2%). Kar et al. [18] also reported a similar effect of beam oscillation on the tensile property of Ti6Al4V. A detailed study of the fractographs of the failed samples was undertaken to understand the mechanism of damage. Figure 7(a-e) shows the fractographs of the failed surfaces under tensile loading of (a) base metal, (b) Joint 1, (c) Joint 2, (d) joint 3, and (e) joint 4. From Fig. 6, it may be noted that the failed surfaces show mixed-mode fracture (combination of cleavage (as shown by arrowhead 1) and dimple (as shown by arrowhead 2)) for all the failed samples.

4 Conclusion

In the present study, the effect of beam oscillation diameter on the microstructure and tensile property of EB-welded CP titanium has been carried out. From the detailed investigations, the following conclusions may be drawn.

1. The microstructure of as-received CP titanium consists of fine equiaxed α -grains. Due to electron beam welding, there is the formation of Widmanstätten martensite and feathery α -titanium phase in the fusion zone. The amount of feathery α -titanium in the weld zone reduces with the increase in beam oscillation diameter.
2. The phase analysis shows the presence of only α -titanium in the weld zone. Lattice strain has reduced after electron beam welding but no trend has been observed with the increase in beam oscillation diameter.
3. Residual stress developed in the fusion zone increases with the increase in beam oscillation diameter which may be attributed to the increased cooling rate associated with beam oscillation.
4. The microhardness study shows an increase in the microhardness of the fusion zone as compared to HAZ and base metal for the samples. The sample welded without beam oscillation has the highest microhardness, and it decreases with the increase in beam oscillation diameter. The sample welded with a maximum oscillation diameter of 1.5 mm shows a minimum microhardness of 250 VHN.
5. Tensile test results show that there is marginal variation in yield strength and UTS as compared to that of as-received CP titanium. The yield strength of the joints varies from 446 to 462 MPa as compared to 465 MPa of base titanium. UTS has also been found to vary from 611 to 623 MPa as compared to 626 MPa of as-received titanium.
6. Percentage elongation is marginally reduced due to EBW and varies from 14 to 18% as compared to 18.2% for as-received alloy. % Elongation increases with the increase in the applied beam oscillation diameter.

7. The fractured surface shows mixed-mode fracture and failure always initiated in the weld zone.

Acknowledgements The authors would like to express appreciation for the support of the technical staff of IIT, Kharagpur in preparing the electron beam-welded CP titanium samples as well as in characterization. The partial financial support from the board of research in nuclear science (BRNS) (to JDM) and the ministry of human resource development (to JS) is gratefully acknowledged. Partial financial support from Alexander von Humboldt Foundation (Friedrich Wilhelm Bessel Award Scheme to JDM) is also gratefully acknowledged. Characterization facility support from the Central Research facility, IIT Kharagpur is fully acknowledged.

Authors' Contributions All authors contributed to the study conception and design. Material preparation, data collection, and analysis were performed by JKS. The first draft of the manuscript was written by JKS and all authors commented on previous versions of the manuscript. All authors read and approved the final manuscript.

Funding The partial financial support from the board of research in nuclear science (BRNS) (to JDM) and the ministry of human resource development (to JS) is gratefully acknowledged. Partial financial support from Alexander von Humboldt Foundation (to JDM) is also gratefully acknowledged.

Availability of Data and Material Data used in the present study are available in the manuscript only. Extra data if required is available on request.

Declarations

Conflict of interest The authors have no competing interests to declare that are relevant to the content of this article.

References

1. Bieler TR, Trevino RM, Zeng L, *Alloys: Titanium, Encyclopedia of Condensed Matter Physics*, Elsevier (2005) 65. ISBN 9780123694010. <https://doi.org/10.1016/B0-12-369401-9/00536-2>
2. Pasang T, Tao Y, Azizi M, Kamiya O, Misiolek W, *MATEC Web of Conferences* **123** (2017) 1. <https://doi.org/10.1051/mateconf/201712300001>
3. Pillai MG, Gupta RK, Pant B, and Sreejith PS, *Trans IIM*, **68** (2015) 423. <https://doi.org/10.1007/s12666-014-0471>
4. Uygur I, and Dogan I, *J Metal* **44** (2005) 19.
5. Danielson P, Wilson R, and Alman D, *Adv Mater Proc* **161** (2003) 39.
6. Won-Bae L, Chang-Young L, Woong-Seong C, Yun-Mo Y, and Seung-Boo J, *Mater Lett* **59** (2005) 3315. <https://doi.org/10.1016/j.matlet.2005.05.064>
7. Mendez PF, Eagar TW, *Adv Mater Process* (2001) 39.
8. Yunlian Q, Ju D, Quan H, Liying Z, *Mater Sci Eng* **280** (2000) pp 177. [https://doi.org/10.1016/S0921-5093\(99\)00662-0](https://doi.org/10.1016/S0921-5093(99)00662-0)
9. Lu W, Shi Y, Lei Y, Li X, *Mater Des* **34** (2012) 509. <https://doi.org/10.1016/j.matdes.2011.09.004>

10. Saresh N, Pillai MG, Mathew J. Investigations into the effects of electron beam welding on thick Ti-6Al-4V titanium alloy. *J Mater. Process. Technol.* 83–8 (2007) 192–193. <https://doi.org/10.1016/j.jmatprotec.2007.04.048>
11. Fu P fei, Mao Z yong, Wang Y jun, Zuo C jin, Xu H Y, *Mater Sci Eng A* **608** (2014) 199. <https://doi.org/10.1016/j.msea.2014.04.048>
12. Wang S, Wu X, *Mater Des* **36** (2012) 663. <https://doi.org/10.1016/j.matdes.2011.11.068>
13. Gupta RK, Anilkumar V, Xavier XR, Ramkumar P, *Mater Today Proc* **5** (2018) 8464. <https://doi.org/10.1016/j.matpr.2017.11.542>
14. Gupta RK, Anil Kumar V, & Xavier XR, *J Mater Eng Perform* **27** (2018) 2192. <https://doi.org/10.1007/s11665-018-3307-9>
15. Wang S, & Wu X, *Mater Des* (1980–2015) **36** (2012) 663. <https://doi.org/10.1016/j.matdes.2011.11.068>
16. Fu P, Mao Z, Zuo C, Wang Y, & Wang C, *Chin J Aeronaut* **27** (2014) 1015. <https://doi.org/10.1016/j.cja.2014.03.020>
17. Dinda SK, Kar J, Jana S, Roy GG, & Srirangam P, *J Mater Process Technol* **265** (2019) 191. <https://doi.org/10.1016/j.jmatprotec.2018.10.026>
18. Kar J, Roy SK, Roy GG, *Int J Adv Manuf Technol* **94** (2018) 4531. <https://doi.org/10.1007/s00170-017-1169-1>
19. Cullity BD, *Elements of X-Ray Diffraction*, 2nd Edition, Addison-Wesley Publishing, 1956, 102 pp, Paperback ISBN 0–201–01174–3.

Publisher's Note Springer Nature remains neutral with regard to jurisdictional claims in published maps and institutional affiliations.

Springer Nature or its licensor (e.g. a society or other partner) holds exclusive rights to this article under a publishing agreement with the author(s) or other rightsholder(s); author self-archiving of the accepted manuscript version of this article is solely governed by the terms of such publishing agreement and applicable law.